International Journal of Engineering Research Updates

Journal homepage: https://orionjournals.com/ijeru/

ISSN: 2783-0187 (Online)

ORION SCHOLAR JOURNALS

(RESEARCH ARTICLE)

Check for updates

Efficacy of the number of plates, fluid flow rate and volume fractions of aluminum oxide nanoparticles on thermal performance of gasket plate heat exchanger

Élcio Nogueira *

Department of Mechanic and Energy, State University of Rio de Janeiro, Brazil.

International Journal of Engineering Research Updates, 2022, 02(01), 025–038

Publication history: Received on 16 January 2022; revised on 27 February 2022; accepted on 01 March 2022

Article DOI: https://doi.org/10.53430/ijeru.2022.2.1.0027

Abstract

The analytical model using the Second Law of Thermodynamics is applied to determine the thermal performance of a gasket plate heat exchanger. The gasket plate heat exchanger under analysis was initially projected for milk pasteurization, with water as a refrigerant, a mass flow rate equal to 0.42 kg/s, and a few plates equal to 20. The present work aims to determine the thermal performance of the heat exchanger, varying the number of plates, the flow rate of the refrigerant fluid, and using nanofluid with variations of volume fractions of aluminum oxide. Thermal efficiency, thermal effectiveness, generation entropy rate, heat transfer rate, and refrigerant and milk outlet temperatures were determined for comparison. In addition, the physical configuration of the plate heat exchanger, concerning the size and heat exchange area of the plates, was maintained.

Keywords: Analytical Method; Gasket Plate Heat Exchanger; Nanofluid; Al_2O_3; Milk Pasteurization

1. Introduction

The second law of thermodynamics is applied to determine the thermal performance of a gasket plate heat exchanger used in milk pasteurization. In addition, a numerical model [1] based on Computational Fluid Dynamic – CFD is used for comparison with a fixed number of plates equal to 20.

Rahul, Nitin Kumar, Vinod Sehrawat, Tarun Gupta, Ravindra Manju, Md. Iqbal Ahmad [1] presents a heat exchange optimization problem for a Gasket Plate Heat exchanger applied in a dairy milk pasteurizing plant. The parameters evaluated during the analysis are the heat transfer area, pressure drop, flow velocity, and thermal efficiency, subject to the number of channels. They apply numerical procedures CFD and compare with experimental tests and analytical approaches. They determine the Reynolds number, Nusselt number, global heat transfer coefficient, and required heat load for a plate number equal to 20. In addition, they present an analysis of the effect of possible fouling on the heat exchanger and state that fouling is much less in a gasket plate heat exchanger than in tubular heat exchangers because of the low fouling rate.

Harshal Khond et al. [2] state that manufacturing companies monopolize plate heat exchanger designs, making it difficult to access vital information related to geometric aspects. They present work whose objective is optimization based on reducing the number of plates using a simple mathematical model. Determine optimal pressure drop and heat capacity solutions based on operational constraints for single-pass and multi-pass. The results show that for a small number of plates, the heat capacity of the exchanger is lower than expected due to poor flow distribution. They conclude that these factors' effect decreases with more plates. However, they note the need for a more complex algorithm that can account for all the complexities associated with the final plate effect, transversal flow distribution, and fouling.

* Corresponding author: Élcio Nogueira
Department of Mechanic and Energy, State University of Rio de Janeiro, Brazil.

Jan Skocilas and Levgen Palaziuk [3] use computational fluid dynamics (CFD) simulation to analyze the turbulent flow heat transfer process in a plate heat exchanger between two chevron plates. A three-dimensional model with the simplified geometry of two crossed corrugated channels provided by chevron plates was designed to study. The three-dimensional numerical model with two corrugated channel geometry uses the k-ω shear stress, transport model, and the essential characteristics of heat exchange and pressure drop were the object of investigation. They carry out a comparative analysis of the literature's analytical and experimental results. In addition, the influence of the angle of inclination was considered, and, as a result, the presence of zones with higher heat losses and low intensity of fluid flow was observed. The simulation results show that chevron plate surface corrugations promote higher heat transfer coefficients and pressure drops. Besides this, the results state that the simulation can help find optimal heat transfer surface geometries with the lowest possible value of hydraulic resistance.

Grigore Roxana et al. [4] state that plate heat exchangers have many advantages and have a high heat exchange area per unit volume, with good heat transfer performance. They cite numerical studies that have been realized to research the fluid flow and heat transfer and present a theoretical and experimental study to this kind of heat exchanger. They used a three-dimensional finite element model to perform a numerical simulation into a counter flow heat exchanger, and the calculation has certain features related to channel geometry. The graphical and numerical results were validated by comparing them with an experimental study. They present a numerical comparison between experimental results, theoretical analysis, and numerical simulation and observe small differences between results. They were justifying that the simplifying assumptions, presence of fouling on the surface of the plates, and a relative degree of uncertainty introduced by the calculation of the convection heat transfer coefficient would be the causes of these differences. Finally, they state that numerical simulation offers a good understanding of the temperature distribution and fluid flow under turbulent motion.

Murat Unverdi and Yasar Islamoglu [5] use a two-dimensional numerical analysis method to investigate plate heat exchanger channels' flow and heat transfer characteristics using aluminum oxide Al_2O_3 and water as the base fluid. They use the finite volume method with the standard k–ε turbulence model for Reynolds numbers equal to 600 and 1900 and volumetric concentrations equivalent to 0.25%, 0.5%, 0.75%, and 1%. Compare with valid experimental results for pure water flow. They concluded that there is good agreement between the numerical model and the experimental results. Furthermore, it was observed that the heat transfer coefficient increases with the increase of the volumetric fraction of the nanofluid and the Reynolds number.

The plate heat exchanger is an example of corrugated walls used for heat transfer enhancement. Dafe Egeregor [6] investigates the heat transfer and pressure drop in a plate heat exchanger using Fluent as the CFD tool and two types of surface geometry: wave geometry and chevron geometry. Water was used as the working fluid with the Reynolds number range between 100 to 25600. He concluded that a suitable choice of plate geometry surface depends on the application.

Fábio A.S. Mota et al. [7] claim that the plate heat exchanger can play an essential role in the face of the growing urgency to save energy and reduce environmental impacts. They list the four main types of PHE's: 1 - gasket, 2 - brazed, 5 - welded, and 6 - semi-welded. The Type 1 Plate Heat Exchanger consists of a package of thin rectangular plates sealed at the edges and held together in a frame. The extensive use of plate heat exchangers is due to advantages such as flexible thermal design, ease of cleaning, and better heat transfer performance. They present two models for optimizing plate heat exchangers. The methods use closed-form equations since a multi-pass PHE consists of sets of single-pass PHEs. They use examples obtained from the literature for analysis and comparisons and observe agreement between effectiveness values. They note that the model using algebraic equations applies only to sufficiently large PHEs and that industrial PHEs have more than 40 thermal plates. They justify the advantage of using an algebraic model for its simplicity.

Anişoara-Arleziana Neagu and Claudia Irina Koncsag [8] mention that empirical, semi-analytical, or theoretical/numerical models were developed to accurately predict the performance of plate heat exchangers to save materials and energy. The work addresses 1 - the modified Lévêque correlation; 2 - the energy losses caused by the reversal of the flow at the edges of the plates; 3 - the change of the flow path caused by the chevron angle. The model was validated under industrial conditions for laminar flow (Re = 8–42) and turbulent flow (Re = 446–1137). In addition, particular values were determined for the inclination angle concerning the vertical direction equal to 30º. They conclude that the generalized Lévêque correlation is reliable.

G. Anusha and P.S. Kishore [9] state that plate heat exchangers provide great heat transfer area concerning the volume and compact heat exchanger. The developed work deals with experimental heat transfer data performed on the plate-type heat exchanger in counter flow arrangement. The heat exchanger consists of 249 plates and has thin metal welded stainless steel plates with 0.5mm thickness; the distance between the two plates is 5mm, and the chevron angle is equal to 60°. The total heat transfer area is 161.62 m^2. The inner hot fluid temperature is 65°C, and the flow rate equals 17.99 kg/s. The cold fluid flow rate is 82366 kg/h and enters at 35°C and leaves at 44.29°C. The correlation was estimated for Nusselt number, and the convective heat transfer coefficient, overall heat transfer coefficient, and exchanger effectiveness were calculated. The numerical and graphical results allowed us to assess the Gasketed Plate heat exchanger's performance.

Ahmad Fakheri [10], Roopesh Tiwari, and Govind Mahesh Wari [11] define thermal efficiency for heat exchangers as an ideal heat exchanger that generates minimum entropy and allows maximum heat exchange, is less irreversible, and provides a new way to design and analyze heat exchangers. This procedure establishes the relationship between effectiveness and efficiency based on thermal irreversibility, which measures the degree of entropy generation in a physical system. It is a new way of analyzing heat exchangers that contrasts with the effectiveness method, which does not provide information on efficiency and irreversibility and uses many unnecessary parameters.

Nogueira, E. [12, 13] applies the thermal irreversibility, efficiency, and effectiveness concepts to analyze heat exchangers. He uses entropy generation rate to determine the global heat transfer coefficient, the transfer unit number – NTU, the actual and maximum heat transfer rate, and outlet temperatures for cold and hot fluids. It demonstrates that it is a simple, efficient, and effective method.

2. Methodology

The problem presented by Rahul et al. [1] deals with optimizing the heat exchange between water and pasteurized milk using a gasket plate heat exchanger where the number of plates was used initially equal to 20. They emphasize the numerical CFD application to design optimization of the pasteurizer plant. The data defined by the authors were used to compare with the application of the analytical methodology presented below

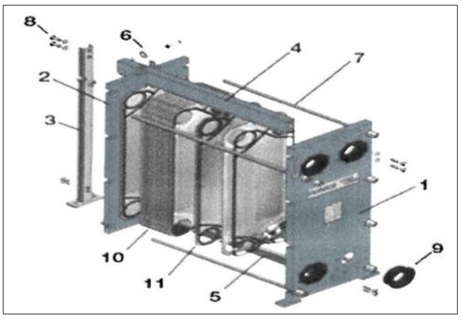

Figure 1 Exploded view of a typical Gasket Plate Heat Exchanger 1 - fixed plate; 2 – pressure plate; 3 -support; 4 – carrying beam; 5 – lower plate guide; 6 – carrying roller; 7 – tightening bolt; 8 – fixing bolt; rubber liner; gasket; heat transfer plate

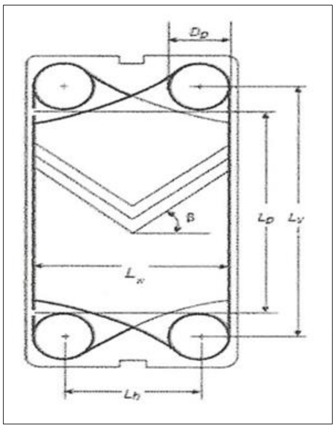

Figure 2 Main dimensions of chevron plate for the projected Gasket Plate Heat Exchanger [1]

Plate Material	SS 304
Plate thickness (mm)	0.6
Chevron angle (degrees)	45
Total number of plates	20
Enlargement factor, ϕ	1.33
Number of passes	One pass/one pass
Overall heat transfer coefficient (clean/fouled) W/m2.k	8,000/4,500
Total effective area (m2)	1.44
All port diameters (mm)	25
Compressed plate pack length, Lc, (m)	0.5
Vertical port distance, L_v, (m)	0.7
Horizontal port distance, L_h, (m)	12.5
Effective channel width, L_w, (m)	15
Thermal conductivity of the plate material (SS304),W/m.K	17.5

Figure 3 Main dimensions for the projected Gasket Plate Heat Exchanger [1]

Table 1 Properties for water (cold), milk (hot), and nanoparticles (Al_2O_3)

	ρ kg/m³	**k W/ (m K)**	**Cp J/ (kg K)**	**μ kg/ (m s)**	**ν m/s²**	**α m/s²**	**Pr**
Water	999.62	0.568	4205.01	$1.38\ 10^{-3}$	$1.38\ 10^{-6}$	$1.35\ 10^{-7}$	10.22
Milk [14,15]	1046.41	0.530	2870	$2.42\ 10^{-3}$	$2.31\ 10^{-6}$	$1.76\ 10^{-7}$	13.12
Al_2O_3	3950	31.92	873.34	-	-	$9.25\ 10^{-6}$	-

$$Th_i = 35\ ºC \ \ldots..(1)$$

$$Tc_i = 1.5\ ºC \ \ldots..(2)$$

Th_i And Tc_i are the hot and cold fluids inlet temperature.

$$\Delta_M = 0.6\ 10^{-3}\ m \ \ldots\ldots.(3)$$

$$k_M = 17.5\frac{W}{m\ K} \ \ldots\ldots\ldots.(4)$$

Δ_M And k_M are the thickness and thermal conductivity of the plate, respectively.

$$N_e = N_t - 2 \ \ldots\ldots\ldots.(5)$$

N_t And N_e are the total number and the effective number of the plates.

$$N_P = 1 \ldots\ldots\ldots.(6)$$

$$N_{CP} = \frac{N_t - 1}{2N_P} \ \ldots\ldots\ (7)$$

N_{CP} Is the number of channels per pass?

$$L_C = 0.50\ m\ \ldots\ldots\ldots\ (8)$$

L_C Is the compressed plate pack length.

$$P_i = \frac{L_C}{N_P}\ \ldots\ldots\ldots..(9)$$

P_i Is the plate pitch.

$$b = P_i - \Delta_M\ \ldots\ldots.(10)$$

b Is the mean channel flow gap.

$$L_W = 0.125\ m\ \ldots\ldots(11)$$

$$L_P = 0.70\ m\ \ldots..(12)$$

L_W And L_P are the horizontal and vertical port distances.

$$A_{Ch} = bL_W\ \ldots\ldots\ldots.(13)$$

A_{Ch} Is the one-channel flow area.

$$A_e = 1.44\ m^2\ \ldots\ldots\ldots.(14)$$

A_e Is the projected total effective area.

$$At_P = L_P\ L_W\ \ldots\ldots..(15)$$

At_P Is the projected plate area.

$$A_1 = \frac{A_e}{N_e}\ \ldots\ldots\ldots.(16)$$

A_1 Is the projected single-plate heat transfer area.

$$\Phi = \frac{A_1}{At_P}\ \ldots\ldots\ldots\ (17)$$

Φ Is the enlargement factor.

$$D_h = \frac{2\ b}{\Phi}\ \ldots\ldots(18)$$

D_h Is the channel hydraulic equivalent diameter

$$N_{CP} = \frac{N_t - 1}{2\ N_P}\ \ldots\ldots\ldots..(19)$$

N_{CP} Is the number of channels per pass?

$$\dot{m}_C = 0.42\frac{Kg}{s}\ldots\ldots\ldots\ldots..(20)$$

$$\dot{m}_h = 0.14\frac{Kg}{s}\ldots\ldots\ldots\ldots.(21)$$

$\dot{m}_C$ And $\dot{m}_h$ are the cold and hot mass flow rate, respectively; $\dot{m}_h$ is fixed in this work.

$$\dot{m}_{Ch} = \frac{\dot{m}_h}{N_{CP}} \; \ldots\ldots\ldots.(22)$$

$$\dot{m}_{Cc} = \frac{\dot{m}_c}{N_{CP}} \; \ldots\ldots\ldots(23)$$

$\dot{m}_{Ch}$ And $\dot{m}_{Cc}$ are the cold and hot mass flow rate per channel.

$$G_{Ch} = \frac{\dot{m}_{Ch}}{A_{Ch}} \ldots\ldots\ldots.(24)$$

$$G_{Cc} = \frac{\dot{m}_{Cc}}{A_{Ch}} \; \ldots\ldots\ldots..(25)$$

G_{Ch} And G_{Cc} are the hot and mass velocity.

The nanofluid properties are given by, where ϕ is the volume fraction of nanoparticle, Nogueira E. [10; 11]:

$$\rho_{nano} = \phi\, \rho_{Particle} + (1-\phi)\rho_W \; \ldots\ldots\ldots.(26)$$

$$\mu_{nano} = \mu_W\, (1 + 2.5\,\phi) \; \ldots\ldots\ldots\ldots\ldots \; (27)$$

$$Cp_{nano} = \frac{\phi\, \rho_{Particle}\, Cp_{particle} + (1-\phi)\, \rho_W\, Cp_W}{\rho_c} \; \ldots\ldots\ldots \; (28)$$

$$k_{nano} = [(k_{Particle} + 2\,k_W + 2\,(k_{Particle} - k_W)\,(1+0.1)^3\phi)/(k_{Particle} + 2\,k_W - (k_{Particle} - k_W)\,(1+0.1)^2\phi)]k_W \; \ldots\ldots\ldots.(29)$$

$$\nu_{nano} = \frac{\mu_c}{\rho_c} \; \ldots\ldots\ldots\ldots \; (30)$$

$$\alpha_{nano} = \frac{k_c}{\rho_c\, Cp_c} \ldots\ldots..(31)$$

$$Pr_{nano} = \frac{\nu_c}{\alpha_c} \; \ldots\ldots\ldots.(32)$$

$$Re_c = \frac{Gc_c D_h}{\mu_c} \; \ldots\ldots..(33)$$

$$Re_h = \frac{Gc_h D_h}{\mu_h} \; \ldots\ldots\ldots..(34)$$

The Nusselt numbers for cold and hot fluids are given by [1, 3, 8]:

$$Nu_c = 0.3\, {Re_c}^{0.663}\, {Pr_c}^{1/3} \; \ldots\ldots..(35)$$

$$Nu_h = 0.3\, {Re_h}^{0.663}\, {Pr_h}^{1/3} \ldots\ldots\ldots.(36)$$

$$h_c = \frac{Nu_c k_c}{D_h} \; \ldots\ldots\ldots\ldots..(37)$$

$$h_h = \frac{Nu_h k_h}{D_h} \; \ldots\ldots\ldots\ldots.(38)$$

h_c And h_h are the convection heat transfer coefficient.

$$Uo = \frac{1}{\frac{1}{\mathrm{h}_c} + \frac{1}{\mathrm{h}_h} + \frac{\Delta_M}{\mathrm{k}_M}} \text{ ………… } (39)$$

Uo Is the overall heat transfer coefficient.

$$C_c = \dot{m}_c\, Cp_c \text{ …… } (40)$$

$$C_h = \dot{m}_h\, Cp_h \text{ …… } (41)$$

C_c And C_h are the cold and hot heat capacities.

$$C^* = \frac{C_{Min}}{C_{Max}} \text{ ……….. } (42)$$

$$NTU = \frac{U_O\, A_e}{C_{Min}} \text{ ………. } (43)$$

NTU Is the number of transfer units?

The thermal effectiveness for the counterflow heat exchanger using the ε-NUT method is given by [4,16,17-18]:

$$\varepsilon_T = \frac{1 - \exp\left(-\mathrm{NTU}\,(1 - \mathrm{C}^*)\right)}{1 + C^* exp\left(-NTU\,(1 - C^*)\right)} \text{ ………. } (44)$$

The thermal efficiency is given by the second law of thermodynamic [10]:

$$\eta_T = \frac{tanh(Fa)}{Fa} \text{ …….. } (45)$$

Fa Is the nondimensional fin analogy number.

From the second law, thermal effectiveness is given as a function of thermal efficiency by:

$$\varepsilon_T = \frac{1}{\frac{1}{\eta_T\, NTU} + \frac{1 + C^*}{2}} \text{ ………… } (46)$$

However, according to Ahmad Fakheri [10], no expression is available for Fa valid for the gasket plate heat exchanger. Therefore, a hybrid solution is chosen using Equations 44 and 46. Finally, the thermal efficiency can be given as a function of thermal effectiveness:

$$\eta_T = \frac{1}{\frac{\mathrm{NTU}}{\varepsilon_T} + \frac{2\,\mathrm{NTU}}{1 + \mathrm{C}^*}} \text{ ………. } (47)$$

$$\dot{Q} = \varepsilon_T\, C_{Min}\, (Th_i - Tc_i) \text{ ……….. } (48)$$

$$\dot{Q}_{Max} = C_{Min}\, (Th_i - Tc_i) \text{ ……… } (49)$$

$\dot{Q}$ And $\dot{Q}_{Max}$ are the actual and maximum heat transfer rate.

$$Th_o = Th_i - \frac{\dot{Q}}{\dot{m}_h Cp_h} \text{ ……… } (50)$$

$$Tc_o = Tc_i + \frac{\dot{Q}}{\dot{m}_c Cp_c} \text{ ……….. } (51)$$

Th_o And Tc_o are the cold and hot outlet temperatures.

$$\sigma_T = \left(\frac{C_h}{C_{Min}}\right) \ln\left(1 - \left(\frac{\left(\frac{Th_i - Tc_i}{Th_i}\right)}{\frac{1}{NTU\ \eta_T \left(\frac{C_{Min}}{C_h}\right)} + \frac{1 + \frac{C_h}{C_c}}{2}}\right)\right) + \left(\frac{C_c}{C_{Min}}\right) \ln\left(1 + \left(\frac{\left(\frac{Thi - Tci}{Tci}\right)}{\frac{1}{NTU\ \eta_T \left(\frac{C_{Min}}{C_c}\right)} + \frac{\left(1 + \frac{C_c}{C_h}\right)}{2}}\right)\right) \ldots\ldots(52)$$

$$\dot{S}_{genT} = \sigma_T C_{Min} \ \ldots.(53)$$

σ_T And $\dot{S}_{genT}$ are the thermal irreversibility and thermal generation entropy rate, respectively [10].

3. Results and discussion

The above methodology allowed heat transfer rate, thermal efficiency, thermal effectiveness, entropy generation rate, and outlet temperatures for water and milk. The initial results address the condition without aluminum oxide nanoparticles dispersed in water. The parameters that undergo variations are the number of heat exchange plates, the water flow, and the volume fraction of the nanoparticles.

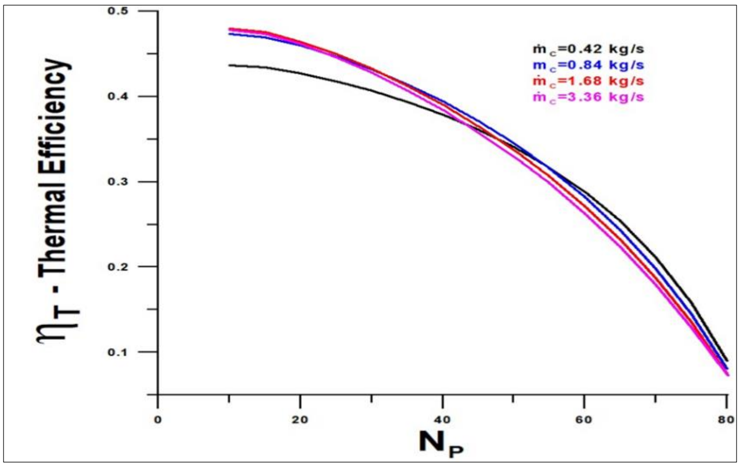

Figure 4 Thermal efficiency versus plate's number for $\boldsymbol{\phi = 0.0}$

Figure 4 shows the thermal efficiency as a function of the number of heat exchanger plates. In general terms, the thermal efficiency is relatively low. Emphasizing the lowest of the flows analyzed when the number of plates is less than 40. Above 40, the thermal efficiency is practically the same for all flows, with slightly higher results for lower flow. For the maximum number of 80 plates, the efficiency is very low, preliminarily indicating that the entropy generation rate is approaching the minimum limit for all flows.

Thermal efficiency, which measures the ratio of current heat transfer rate to maximum heat transfer rate, increases with increasing water flow. However, it is relatively low, less than 40%, for plate numbers less than 40. Figure 5 shows that the heat exchange tends to a maximum for about 80 plates, as expected, according to the minimum obtained for efficiency. That is, the effectiveness approaches 100%. In this case, the water flow practically does not influence the result of the heat exchange.

Figure 6 presents the current, and maximum heat transfer rate results as a function of the number of plates and water flow variation. Higher water flow rates allow greater heat exchange between the fluids for plate numbers lower than 80. At the limit, close to 80 plates, the heat transfer rates are the same for all flows and present results very close to the maximum. Therefore, it is advantageous to increase the water flow of plates lower than 60.

The rate of entropy generation is shown in Figure 7 – the rate of entropy generation increases with an increasing number of plates and increasing water flow. The variation in the entropy generation rate is relatively high for smaller numbers of plates and tends to stabilize around 80 plates, which corroborates all the previous analyses.

Figure 8 presents values for the refrigerant outlet temperature as a function of the number of plates and the water flow. The outlet temperature increases with the number of plates and presents higher values for lower water flows. The result is justified because there is a greater heat exchange area with more plates and a lower thermal capacity for lower flow rates. Thus, lower internal energy absorption for low water flow, enabling higher outlet temperatures.

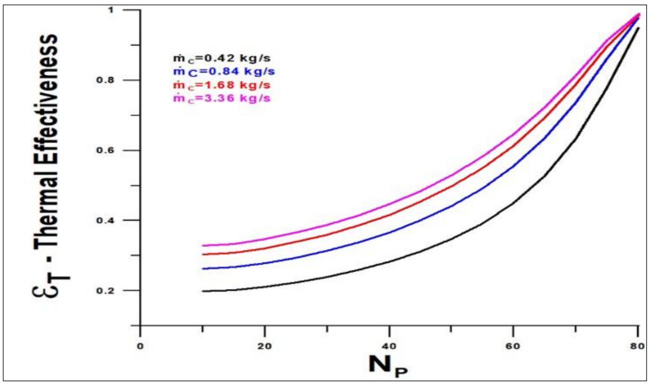

Figure 5 Thermal effectiveness versus plates number for $\boldsymbol{\phi = 0.0}$

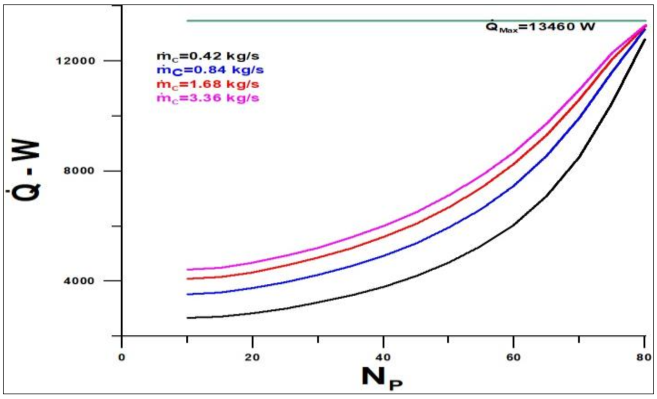

Figura 6 Heat transfer rate versus plates number for $\boldsymbol{\phi = 0.0}$

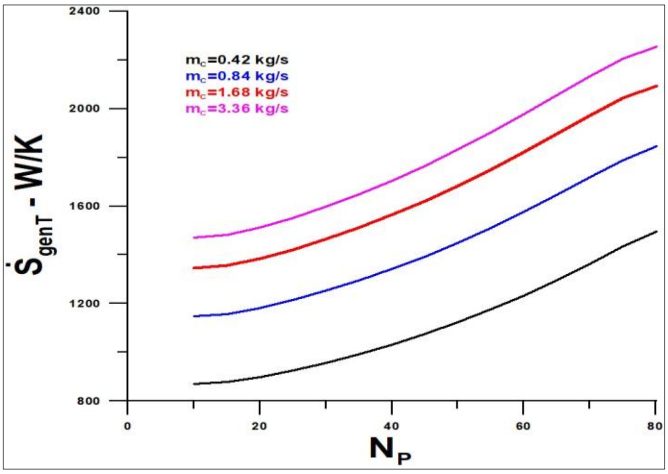

Figura 7 Entropy generation rate versus plate's number for $\boldsymbol{\phi = 0.0}$

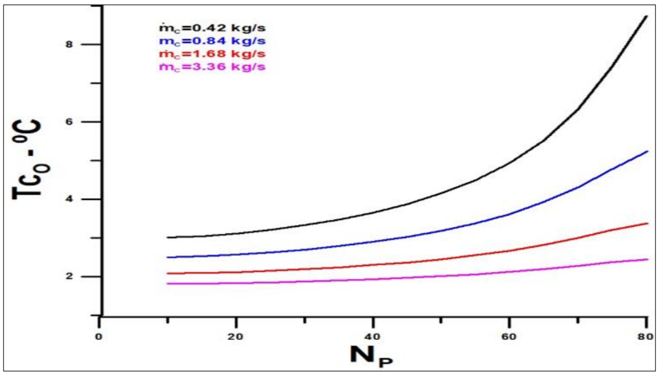

Figura 8 Water outlet temperature versus plate's number for $\boldsymbol{\phi = 0.0}$

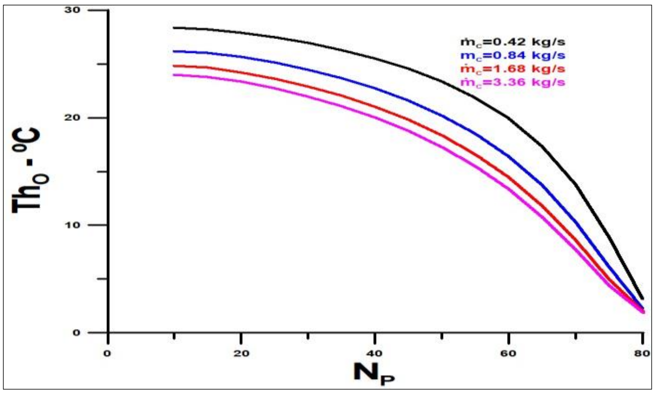

Figura 9 Milk outlet temperature versus plate's number for $\boldsymbol{\phi = 0.0}$

Figure 9 shows that the milk outlet temperature drops significantly as the number of plate's increases and the water flow rate increases. A greater number of plates means a greater area of heat exchange between the fluids, which lowers the temperature of the hot fluid. In turn, higher flow rates of the cold fluid allow an increase in the thermal capacity and consequent better absorption of energy in the form of heat from the hot fluid, leading to lower outlet temperatures. A relevant fact is that the number of plates equal to 80 leads to the limit situation regardless of the flow rate of the cold fluid, with the minimum outlet temperature of the hot fluid tending asymptotically towards the inlet temperature of the cold fluid. Above this value, there is no justification for increasing the number of plates and cold fluid flow. However, the results indicate that for flows lower than 0.42 kg/s, the maximum number of plates can be higher than 80.

Figures 10 – 15 present results for Nano fluid composed of water as base fluid and aluminium oxide nanoparticles.

The volume fractions of nanoparticles are relatively high, equal to 0.10 and 0.20. The flow rates for the Nano fluid are equal to 0.42 kg/s and 3.36 kg/s. The number of plates varies from 10 to 80. With the increase in the volume fraction, the Nano fluid specific heat plays a fundamental role in the results.

Figure 10 shows the thermal efficiency as a function of the number of heat exchanger plates with variations in the Nano fluid flow rate and the nanoparticles' volumetric fraction. Thermal efficiency is relatively low and decreases significantly with volume fraction for lower Nano fluid mass flow. For higher flow rates of Nano fluids, the nanoparticles practically do not affect the efficiency. In this case, the efficiency parameters are the flow rate and the number of plates. For high plate numbers, Nano fluid flow rates also do not affect efficiency.

Figure 11 shows the thermal efficiency results as a function of the number of heat exchanger plates with variations in the Nano fluid flow rate and the nanoparticles' volumetric fraction. Efficacy decreases with increasing nanoparticle volume fraction at low Nano fluid flow rates. For high flow rates, however, the variation in the volumetric fraction of the nanoparticles practically does not affect the thermal efficiency. Therefore, it can be anticipated that the heat exchange between the fluids decreases significantly with the inclusion of nanoparticles at low flow rates of the Nano fluid.

The results in Figure 12 corroborate the conclusions previously issued: for low flow rates of the Nano fluid, the inclusion of nanoparticles decreases the rate of heat exchange between the fluids. However, for high flow rates and high plate numbers, the influence of nanoparticles is practically null.

Figure 13 shows that the entropy generation rate increases with the Nano fluid flow and the number of plates. However, the inclusion of nanoparticles increases the thermal capacity of the Nano fluid, and they absorb part of the energy exchanged between the fluids, decreasing the rate of entropy generation. The influence of nanoparticles decreases with the increasing flow rate of the Nano fluid since their impact on heat capacity decreases.

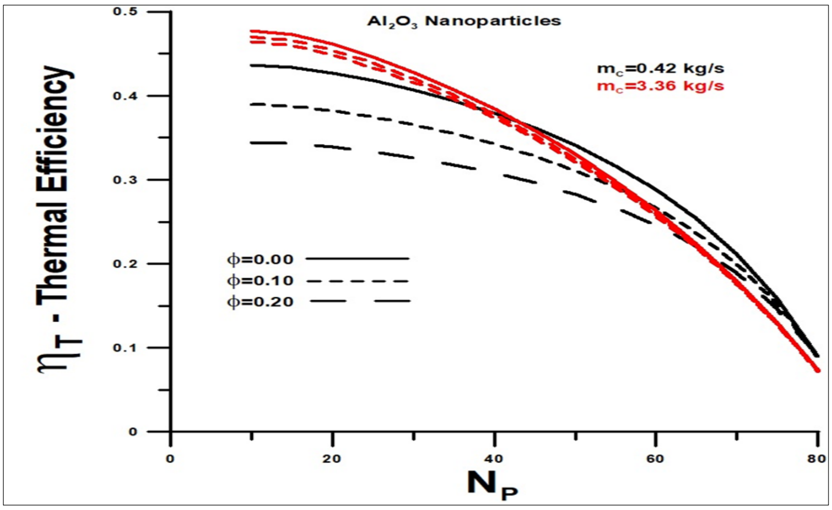

Figure 10 Thermal efficiency versus plates number for ϕ=0.10 and ϕ=0.20

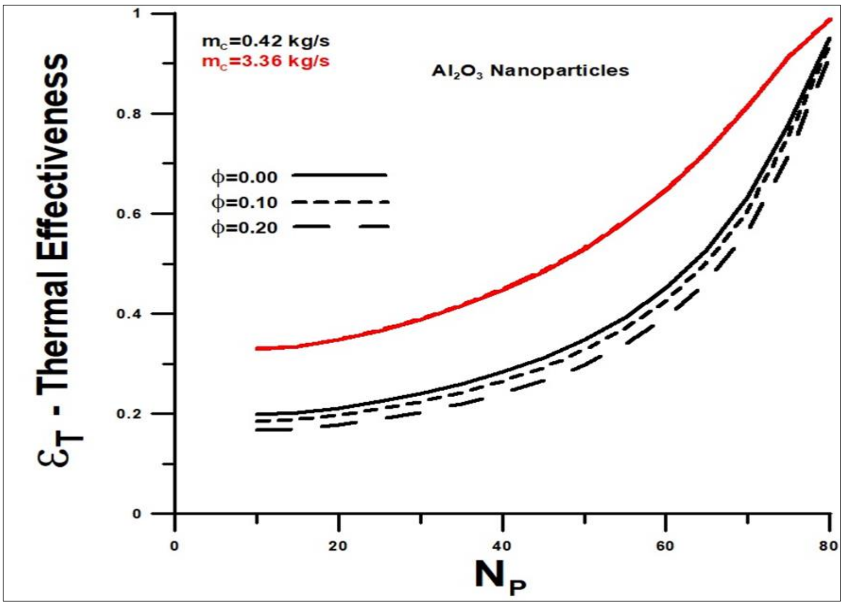

Figure 11 Thermal effectiveness versus plates number for ϕ=0.10 and ϕ=0.20

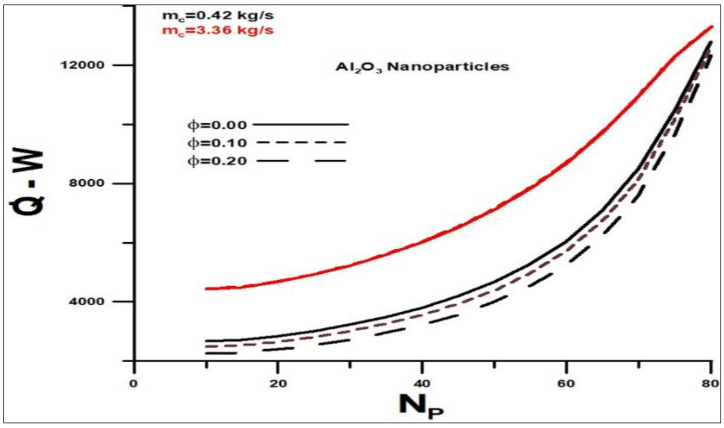

Figura 12 Heat transfer rate versus plates number for $\boldsymbol{\phi}$=0.10 and $\boldsymbol{\phi}$=0.20

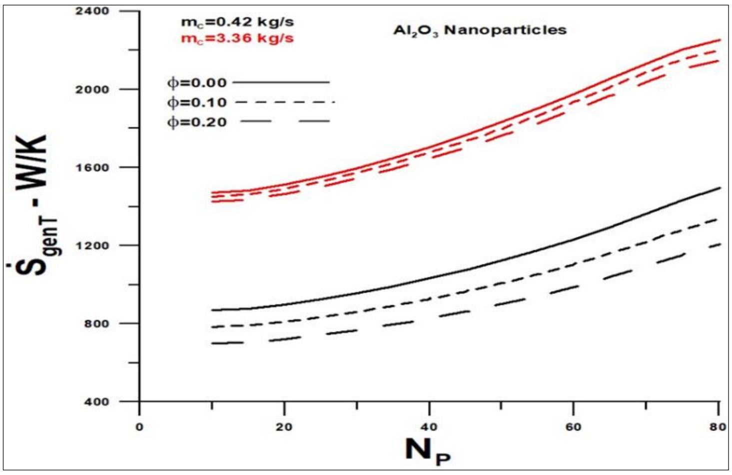

Figura 13 Entropy generation rate versus plates number for $\boldsymbol{\phi}$=0.10 and $\boldsymbol{\phi}$=0.20

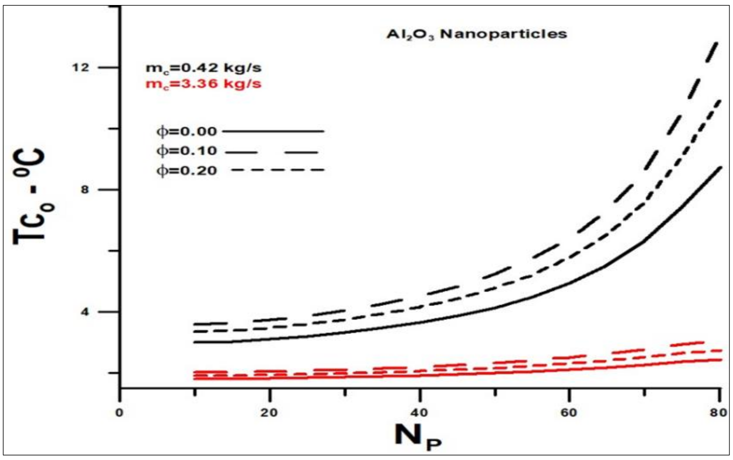

Figura 14 Water outlet temperature versus plates number for $\boldsymbol{\phi}$=0.10 and $\boldsymbol{\phi}$=0.20

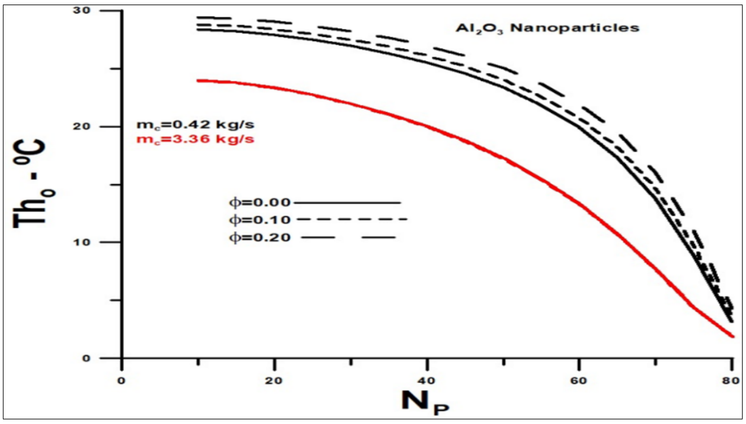

Figura 15 Milk outlet temperature versus plates number for ϕ=0.10 and ϕ=0.20

The water and milk outlet temperatures are shown in Figure 14 and Figure 15, respectively.

In water, in Figure 14, nanoparticles contribute to greater energy absorption in the form of heat and a higher outlet temperature. The contribution to the temperature variation is more significant for smaller flows when the increase in the thermal capacity has a greater relative weight. This contribution to a higher heat capacity is relatively more minor at higher flow rates, contributing to a less significant increase in the outlet temperature.

In milk, Figure 15, the outlet temperature is slightly higher than when the milk exchanges heat with pure water. It can be seen, in Figure 12, that the heat transfer rate drops with the introduction of nanoparticles fractions, and this is reflected in the milk outlet temperature. The outlet temperature of milk does not change when nanoparticles are introduced into the water for high flow rates.

In practical terms, within the range of flow rates analyzed, the introduction of nanoparticles has no advantage when a lower outlet temperature is required for the milk.

4. Conclusion

Analysis of heat transfer between water and pasteurized milk was performed using a gasket plate heat exchanger with plate number equal to 20 and water flow rate equal to 0.42 kg/s as a parameter. The number of plates was changed in the study, varying between 10 plates and the smallest number of plates that allowed the highest heat transfer rate between the media. Furthermore, for analysis purposes, aluminium oxide nanoparticles were introduced into the water, with volume fractions equal to 0.10 and 0.20.

The conclusions that were reached:

- The thermal efficiency is low and decreases with the increase of water flow and the introduction of aluminium oxide nanoparticles fractions.
- Regardless of the water flow rate and the volume fractions of the nanoparticles, the thermal efficiency tends to a minimum when the number of plates is equal to 80.
- The thermal effectiveness increases with the water flow. However, with the increase of the number of plates, it decreases with the introduction of nanoparticles. In this case, the decrease is more significant for low water flows.
- The effectiveness tends to 1.0 when the number of plates approaches 80. In this case, it does not depend on the water flow and the volumetric fraction of the nanoparticles.
- The heat transfer rate increases with the water flow. The increase in the number of plates decreases with the introduction of nanoparticles. In this case, the decrease is more significant for low water flows.
- The heat transfer rate tends to the maximum possible for the configuration under analysis when the number of plates approaches 80, regardless of the water flow and the variation in the fraction of aluminium oxide nanoparticles.

- The analysed heat exchanger has maximum performance for several plates equal to 80, regardless of the water flow and the volume fraction of the nanoparticles.
- The parameter that determines optimal thermal performance is the number of plates.

References

[1] Rahul, Nitin Kumar, Vinod Sehrawat, Tarun Gupta, Ravindra Manju, Md. Iqbal Ahmad. Design Analysis of Gasketed Plate Heat Exchanger. International Journal for Technological Research in Engineering. May 2017; 4(9).

[2] Harshal Khond, Dilpak Saurabh P, Kundalik V, Mali. Design Optimization Algorithm for Plate Heat Exchanger. International Journal of Current Engineering and Technology, MIT College of Engineering, Pune, India, AMET 2016, INPRESSCO IJCET Special Issue-4 (March 2016).

[3] Jan Skocilas, Levgen Palaziuk. CFD Simulation of the Heat Transfer Process in a Chevron Plate Heat Exchanger Using the SST Turbulence Model. Czech Technical University in Prague, Acta Polytechnica. 2015; 55(4): 267–274.

[4] Grigore Roxana, Popa Sorin, Hazi Aneta and Hazi Gheorghe. Study Regarding Numerical Simulation of Counter Flow Plate Heat Exchanger. Numerical Analysis - Theory and Application, Prof. Jan Awrejcewicz (Ed.). 2011; ISBN: 978-953-307-389-7, InTech.

[5] Murat Unverdi and Yasar Islamoglu. Numerical Investigation of Forced Convection Heat Transfer Performance of Al2O3/Water Nanofluids in Plate Heat Exchanger Channel. Proc. of the International Conference on Advances in Mechanical and Automation Engineering - MAE 2016.

[6] Dafe Egeregor. Numerical Simulation of Heat Transfer and Pressure Drop in Plate Heat Exchanger Using Fluent as a CFD Tool. Master's Degree Thesis, Department of Mechanical Engineering, Blekinge Institute of Technology, Karlskrona, Sweden. 2008.

[7] Fábio AS, Mota, EP, Carvalho, Mauro ASS. Ravagnani. Modeling and Design of Plate Heat Exchanger. Heat Transfer Studies and Applications, Chapter. 2015; 7: 165-199.

[8] Anişoara-Arleziana Neagu and Claudia Irina Koncsag. Model Validation for the Heat Transfer in Gasket Plate Heat Exchangers Working with Vegetable Oils. Processes. 2022; 10: 102.

[9] G Anusha, PS Kishore. Heat Transfer Analysis of Gasketed Plate Heat Exchanger. International Journal of Engineering Research. 2016; 5(12): 943-947.

[10] Ahmad Fakheri. Heat Exchanger Efficiency. Transactions of the ASME. 2007; 129: 1268- 1276.

[11] Tiwari R, Maheshwari G. Effectiveness and efficiency analysis of parallel flow and counter flow heat exchangers. IJAIEM. 2017; 6: 314-319.

[12] Nogueira E. Thermal performance in heat exchangers by the irreversibility, effectiveness, and efficiency concepts using nanofluids. Journal of Engineering Sciences. 2020; 7: F1-F7.

[13] Nogueira E. Efficiency and Effectiveness Method versus ε-NTU Method with Application in Finned Flat Tube Compact Heat Exchanger with Water-Ethylene Glycol as Nanofluid Base of Iron Oxide Nanoparticles. 2022.

[14] Peter Hlaváč, Monika Božiková. Effect of Temperature on Milk Rheologic and Thermophysical Properties. Journal on Processing and Energy in Agriculture. 2011; 15: 1.

[15] Biblid: 1821-4487 (2011) 15; 1; p.17-22. UDK: 591.146:621.3.017

[16] Alcântara, Lizzy Ayra Pereira; Fontan, Rafael da Costa Ilhéu; Bonomo, Renata Cristina Ferreira; Souza, Jr., Evaldo Cardozo de; Sampaio, Vanessa Santos; and Pereira, Rúbner Gonçalves. Density and Dynamic Viscosity of Bovine Milk Affect by Temperature and Composition. International Journal of Food Engineering. 2012; 8(1). Article 11.

[17] Kays WM, London AL. Compact Heat Exchangers. MacGraw-Hill, New York. 1984.

[18] Sadik Kakaç, Hontang Liu, Anchasa Pramuanjaroenkij. Heat Exchangers – Selection, Rating, and Thermal Design. Third Edition, CRC Press, Taylor & Francis Groupe, Boca Raton, London, New York. 2012.